RSC Advances

PAPER

View Article Online
View Journal | View Issue

Cite this: *RSC Adv.*, 2015, **5**, 69782

Two-step spin crossover behaviour in the chiral one-dimensional coordination polymer $[Fe(HAT)(NCS)_2]_\infty$†

Tania Romero-Morcillo,[a] Francisco J. Valverde-Muñoz,[a] M. Carmen Muñoz,[b] Juan Manuel Herrera,[c] Enrique Colacio[c] and José A. Real*[a]

Solvated and unsolvated forms of the complex $[Fe(HAT)(NCS)_2]_\infty \cdot (n\text{MeOH})$ (**1**) (n = 1.5, 0; HAT = 1,4,5,8,9,12-hexaazatriphenylene) were prepared. The structure of **1·(1.5MeOH)**, measured at 120 K, showed that this system crystallizes in the homochiral $P4_3$ tetragonal space group. The solid is constituted of stacks of one-dimensional coordination polymers running along c-axis. All the Fe^{II} centres have the same Λ or Δ conformation and are in the LS state at 120 K. In the range of temperatures 10–300 K the magnetic properties of **1·(1.5MeOH)** shows the occurrence of reversible spin crossover behaviour. However, above *ca.* 310 K complete desolvation of **1·(1.5MeOH)** to give **1** was observed from crystal structure analysis, magnetic behaviour and thermal analysis. Compound **1** displays a two-step spin crossover behaviour characterised by a plateau 60 K wide. Simulation of the two-step behaviour in the frame of the regular solutions theory afforded, respectively, the critical temperatures (T_{ci}), the interaction parameters (Γ_i), and the enthalpy (ΔH_i) and entropy (ΔS_i) variations for steps i = 1 and 2: $T_{c1}(T_{c2})$ = 172 (358) K, $\Gamma_1(\Gamma_2)$ = 1.6 (3.0) kJ mol^{-1}, $\Delta H_1(\Delta H_2)$ = 5.7 (18.3) kJ mol^{-1} and $\Delta S_1(\Delta S_2)$ = 33.4 (51.0) J K mol^{-1}.

Received 9th July 2015
Accepted 10th August 2015

DOI: 10.1039/c5ra13491a

www.rsc.org/advances

Introduction

Fe^{II} spin crossover (SCO) complexes switch between the high (S = 2, HS) and low (S = 0, LS) spin states in response to external stimuli such as temperature, pressure, light and analytes. This spin state switch involves an internal electron transfer between the e_g and t_{2g} orbitals of the Fe^{II} and simultaneous changes in magnetic, optical, dielectric and structural properties.[1]

These appealing intrinsic properties confer to the SCO phenomenon a multidisciplinary character. For example, the search for strong cooperative SCO transitions has inspired chemists the synthesis of a great variety of SCO complexes of different dimensionalities ranging from discrete zero-dimensional to three-dimensional coordination polymers.[1,2] Rationalisation of the cooperative nature of the SCO has resulted to be for physicists an excellent platform to test general theories for phase transitions.[3] The search for new functional materials has prompted to investigate synergies between thermo-, piezo-, and/or photo-induced SCO behaviour and other interesting phenomena, *i.e.* magnetic coupling,[4] magnetic ordering,[5] electrical conductivity,[6] luminescence,[7] porosity (host–guest chemistry),[8] melting (*i.e.* liquid crystals),[9] *etc.* Most of this work has created application expectancies in the area of sensors and memory devices and have motivated in the past years important activity about processing of SCO Fe^{II} materials at micro-, nano- and molecular scales.[10]

In this context, we have decided to explore the possibilities of the ligand 1,4,5,8,9,12-hexaazatriphenylene (HAT) in the synthesis of new Fe^{II} SCO complexes. HAT (Scheme 1) is an appealing highly symmetric tris-chelate bidentate ligand that can afford discrete trinuclear species and one-, two- and three-dimensional coordination polymers.[11] Nevertheless, a relative small number of complexes with first-row transition metal ions have been reported until now. Likely, the inherent difficulties associated with several-steps low yield synthetic route together with low solubility are the main reasons that explain this situation. As far as we know, only five works dealing with magnetically relevant M^{II} = Fe,[12] Co[13] and Cu[14] complexes have been reported. In these cases, HAT acts as a tris-bidentate or bis-bidentate chelate and the coordination sphere of M^{II} is completed with ancillary weak-field ligands (H_2O, CH_3OH, Cl^-, SO_4^{2-}, *etc.*) giving trinuclear $[M^{II}{}_3HAT]$ or binuclear $[M^{II}{}_2HAT]$ species, which in some instances are connected by the ancillary ligands affording infinite chains. The magnetic coupling through HAT ligand has been demonstrated to be quite small.

[a]*Instituto de Ciencia Molecular (ICMol), Universidad de Valencia, 46980 Paterna, Valencia, Spain. E-mail: jose.a.real@uv.es*

[b]*Departamento de Física Aplicada, Universitat Politècnica de València, 46022, Valencia, Spain*

[c]*Departamento de Química Inorgánica, Universidad de Granada, Avda. Fuentenueva s/n, 18071, Granada, Spain*

† Electronic supplementary information (ESI) available. CCDC 1060123. For ESI and crystallographic data in CIF or other electronic format see DOI: 10.1039/c5ra13491a

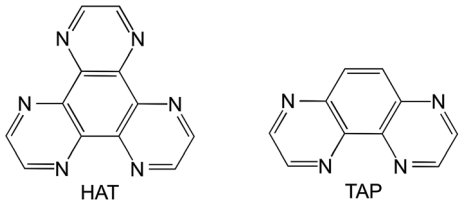

Scheme 1 Representation of HAT and TAP ligands.

Similarly to *o*-phenanthroline (phen) or 2,2′-bipyridine (2,2′-bpy) ligands, the α-diimine functions of HAT generate medium-strong ligand field strength in the Fe^{II} coordination sphere. Thus, combining the Fe^{II}–HAT system with more appropriate ancillary ligands like NCS^- could potentially afford polynuclear and polymeric SCO complexes. This is supported by the related SCO complex $[Fe(TAP)_2(NCS)_2]\cdot CH_3CN$ where TAP is 1,4,5,8-tetraazaphenanthrene, which could formally be described as a fragment of the HAT ligand (see Scheme 1).[15]

Here we describe the synthesis, crystal structure and magnetic behaviour of the chiral one-dimensional coordination polymer $[Fe(HAT)(NCS)_2]_n\cdot 1.5CH_3OH$ [**1·(1.5MeOH)**] and its desolvated derivative (**1**), which represent the first examples of SCO in the Fe^{II}–HAT system.

Results and discussion

Synthesis

1·(1.5MeOH) was synthesised as dark-blue (almost black) needles by slow diffusion methods in a mixture of dichloromethane/methanol. The chemical formula of **1·(1.5MeOH)** was established from single crystal X-ray diffraction and thermogravimetric analysis. Consistently with the X-ray structure and the magnetic behaviour, the thermogravigram of **1·(1.5MeOH)** showed desorption of 1.5 molecules of methanol in the temperature interval 305–380 K (see Fig. S1 ESI†). The resulting desolvated compound **1** showed remarkable thermal stability in the temperature interval 380–580 K. Elemental chemical analysis confirmed the chemical formula of **1**.

Crystal structure of 1·(1.5MeOH)

Due to loss of solvent molecules at about 300 K, the crystal structure of **1·(1.5MeOH)** was measured only at 120 K. It crystallises in the chiral $P4_3$ tetragonal space group. A selection of crystal data and bond lengths and angles of the coordination core $[FeN_8]$ are gathered in Tables 1 and 2, respectively. Fig. 1a shows an ORTEP representation of the asymmetric unit together with the atom numbering. The Fe^{II} is surrounded by two crystallographically equivalent HAT ligands and two crystallographically distinct NCS^-, which adopt a *cis* conformation and define a $[FeN_6]$ distorted octahedral site. The Fe–N bond lengths are in the range 1.940(6)–2.015(5) Å. The sum of the deviations from the ideal octahedron of the 12 "*cis*" N–Fe–N angles $\left(\Sigma = \sum_{i=1}^{12} |\theta_i - 90|\right)$ shows that the coordination centre is slightly distorted with Σ value equal to 33°, while the average of the trigonal distortion angle $\left(\Phi = \sum_{i=1}^{24}(|\phi_i - 60|)/24\right)$ defined by superposition of two opposite triangles of the octahedron has been estimated to be 3.53°. Comparison of these values with those observed for related SCO complexes[16] (see Table 3) and the observed Fe–N bond lengths indicate that **1·(1.5MeOH)** is in the LS state at 120 K.

The Fe–NCS linkages, Fe–N(5)–C(13) = 175.9(7)° and Fe–N(6)–C(14) = 171.1(18)° are slightly bent. The thiocyanate group N(5)–C(13)–S(1) is essentially linear (178.8(11)°), in contrast to the other thiocyanate (N(6)–C(14)–S(2)) whose sulphur atom was found to be strongly disordered and had to be modelled in two positions.

The HAT ligand acts as a bis-bidentate ligand through the α-diimine moieties N(1)–C(2)–C(3)–N(2) and N(3)–C(10)–C(11)–N(4) defining infinite chains generated by a four-fold helicoidal axis sited along *c*-direction (Fig. 1b). Given the lack of inversion symmetry in the crystal all chains turn in the same direction rendering chirality to the crystal. The separation between the Fe^{II} ions through HAT is 6.737(2) Å.

Fig. 2 displays the crystal packing represented by four chains running along *c*-direction. Equivalent Fe^{II} atoms of adjacent chains are separated by $a = b = 8.5067(4)$ Å. No relevant short contacts (smaller than the sum of the corresponding van der Waals radii) were found between adjacent chains. The particular disposition of the chains defines a channel in the middle of the unit cell where two crystallographically distinct MeOH molecules are located (with occupancies 1 and 0.5 for $H_3C(15)$–O(1)–H and $H_3C(16)$–O(2)–H, respectively). Short contacts (C···O, C···C and C···S), smaller than the sum of the van der Waals radii (*ca.* 3.25, 3.70 and 3.70 Å, respectively), are observed between the methanol molecule $H_3C(15)$–O(1)–H and the moieties [N(1)C(1)C(2)C(11)C(12)N(4)], [N(1)C(1)C(2)C(11)C(12)N(4)] and N(6)–C(14)–N(2,2A): $O(1)\cdots C(12)^i = 3.193(8)$ Å and $O(1)\cdots C(1)^{ii} = 3.124(9)$ Å, $O(1)\cdots C(7)^i = 3.144(10)$ Å, $C(15)\cdots C(7)^i = 3.52(2)$ Å, $C(15)\cdots C(14)^{ii} = 3.64(2)$ Å ($i = -y, x+1, z-1/4$; $ii =$

Table 1 Crystal data of compound **1·(1.5MeOH)** ($T = 120$ K)[a]

Empirical formula	$C_{15.5}H_{12}O_{1.5}N_8S_2Fe$
Mr	454.30
Crystal system	Tetragonal
Space group	$P4_3$
a (Å)	8.5067(4)
c (Å)	26.288(2)
V (Å^3)	1902.3(2)
Z	4
D_c (mg cm^{-3})	1.586
F (000)	924
μ (Mo-K$_\alpha$) (mm^{-1})	1.040
Crystal size (mm)	0.06 × 0.06 × 0.15
Temperature (K)	120(1)
No. of total reflections	3520
No. of reflections [$I > 2\sigma(I)$]	3062
R_1 [$I > 2\sigma(I)$]	0.0645
R_1 [all data]	0.0753
S	0.0942

[a] $R_1 = \Sigma||Fo| - |Fc||/\Sigma|Fo|$; $wR = [\Sigma[w(Fo^2 - Fc^2)^2]/\Sigma[w(Fo^2)^2]]^{1/2}$ $w = 1/[\sigma^2(Fo^2) + (mP)^2 + nP]$ where $P = (Fo^2 + 2Fc^2)/3$; $m = 0.1689$; $n = 16.9868$.

Table 2 Selected bond lengths [Å] and angles [°] for **1·(1.5MeOH)** ($T = 120$ K)

Fe–N(1)	1.993(6)
Fe–N(2)	2.005(5)
Fe–N(3)	2.015(5)
Fe–N(4)	1.980(6)
Fe–N(5)	1.946(5)
Fe–N(6)	1.940(6)
N(1)–Fe–N(2)	82.6(2)
N(1)–Fe–N(3)	93.3(2)
N(1)–Fe–N(4)	176.2(2)
N(1)–Fe–N(5)	90.8(2)
N(1)–Fe–N(6)	91.9(2)
N(2)–Fe–N(3)	88.9(2)
N(2)–Fe–N(4)	96.2(2)
N(2)–Fe–N(5)	173.0(3)
N(2)–Fe–N(6)	91.4(2)
N(3)–Fe–N(4)	83.0(2)
N(3)–Fe–N(5)	89.2(2)
N(3)–Fe–N(6)	174.8(2)
N(4)–Fe–N(5)	90.2(2)
N(4)–Fe–N(6)	91.8(2)
N(5)–Fe–N(6)	91.1(3)

$x - 1, y, z$). The thermally disordered methanol molecule $H_3C(16)$–O(2)–H is more weakly fastened to the chains, only two contacts are observed: C(16)···C(4) = 3.70(2) Å, C(16)···C(5) = 3.71(2) Å and C(16)···C(9) = 3.60(2) Å.

Magnetic properties

The magnetic properties are shown in Fig. 3 in the form of the product $\chi_M T$ *versus* T (χ_M is the molar magnetic susceptibility and T is temperature). The $\chi_M T$ product of freshly prepared **1·(1.5MeOH)** crystals is about 1.59 cm^3 K mol^{-1} a value which denotes the occurrence of *ca.* 50 : 50 population of the LS and HS spin states at 300 K. $\chi_M T$ decreases on cooling down to 50 K to reach a value of 0.20 cm^3 K mol^{-1} and suggests practically complete transformation of the HS Fe^{II} centres to the LS state. The $\chi_M T$ *vs.* T curve perfectly matches the cooling mode upon heating up to 300 K indicating that no thermal hysteresis is present. In the temperature range 306–312 K the slope of the $\chi_M T$ *vs.* T plot increases noticeably and decreases again in the temperature range 312–400 K. Consistently with the thermogravimetric analysis, this increase of $\chi_M T$ has been associated with the lost of the methanol molecules to give **1**. At 400 K the $\chi_M T$ value is *ca.* 3 cm^3 K mol^{-1} indicating that the SCO is not completed at this temperature. Afterwards, the magnetic behaviour of **1** was successively recorded cooling from 400 K down to 10 K. In the temperature range 400–312 K, $\chi_M T$ matches reasonably well the previous heating, but notably differs at lower temperatures showing the occurrence of a two-step transition characterised by a plateau *ca.* 60 K wide in the interval 285–225 K. This magnetic behaviour was repeated three cycles obtaining reproducible data (see Fig. S2 in ESI†).

Assuming that the two-step transition is the result of two independent one-step events, we have simulated the experimental data using the regular solution model proposed by Slichter–Drickamer:[17]

$$\ln\left[\frac{1-\gamma_{HSi}}{\gamma_{HSi}}\right] = \frac{\Delta H_i + \Gamma_i\,(1-2\gamma_{HSi})}{RT} - \frac{\Delta S_i}{R};\ i = 1,\ 2 \qquad (1)$$

where γ_{HSi} is the HS molar fraction, ΔH_i and ΔS_i are, respectively, the enthalpy and entropy variations during the SCO, Γ_i represents the interaction energy between molecules (cooperativity) of the step i and R is the ideal gas constant. The quantity γ_{HSi} can be expressed as a function of the $\chi_M T$ product as follows:

$$\gamma_{HSi} = \frac{(\chi_M T)_{mi} - (\chi_M T)_{LSi}}{(\chi_M T)_{HSi} - (\chi_M T)_{LSi}} \qquad (2)$$

where $(\chi_M T)_{mi}$ represents the $\chi_M T$ value in the temperature interval 0–260 K for step 1 and 260–475 K for step 2, $(\chi_M T)_{HSi}$ and $(\chi_M T)_{LSi}$ represent the $\chi_M T$ values for 100% populated HS and LS species for each step. $(\chi_M T)_{LS1}$ has been considered equal to 0 cm^3 K mol^{-1} while $(\chi_M T)_{LS2} = (\chi_M T)_{HS1} = 1/2(\chi_M T)_{HS2}$. The experimental data has been simulated using T_{ci} ($= \Delta H_i/\Delta S_i$), ΔS_i and Γ_i as adjustable parameters. T_{ci} represents the equilibrium temperature at which $\gamma_{LSi} = \gamma_{HSi} = 0.5$ where the Gibbs free energy $\Delta G_i = 0$. As can be seen in Fig. 3 experimental (open circles) and calculated (red line) $\chi_M T$ *vs.* T plots agree satisfactorily for $T_{c1}(T_{c2}) = 172$ (358) K, $\Gamma_1(\Gamma_2) = 1.6$ (3.0) kJ mol^{-1}, $\Delta S_1(\Delta S_2) = 33.4$ (51.0) J K mol^{-1}, $(\chi_M T)_{HS1}((\chi_M T)_{HS2}) =$ 1.7 (3.4) cm^3 K mol^{-1}. The calculated ΔH_1 and ΔH_2 values are 5.7 and 18.3 kJ mol^{-1}, respectively. The total ΔS_T and ΔH_T variations, 84.4 J K mol^{-1} and 24 kJ mol^{-1} respectively, are reasonable taking into account the high T_{c2} value.[18] In the frame of the mean field theory here employed, the cooperativeness, expressed as $C_i = \Gamma_i/2RT_{ci}$, shows that both steps have essentially the same small cooperative nature ($C_1 = 0.6$ and $C_2 = 0.5$).

Discussion

The coordination mode of the discrete $[Fe(HAT)_2(NCS)_2]$ moiety in **1·(1.5MeOH)** is similar to that observed for related mononuclear $[Fe(L)_2(NCS)_2]$ species where L is a bidentate α-diimine ligand of the type phen,[16a] 2,2′-bipy,[16d] btz (2,2′-bi-4,5-dihydrothiazine),[16b] bt (bithiazoline, polymorph A)[16e] or the closely related TAP ligand[15] (see Scheme 1). In all these examples the ligands coordinate the Fe^{II} in a *cis* configuration. The average Fe–N bond length of **1·(1.5MeOH)**, equal to 1.980 Å at 120 K, compares well with that found for the mononuclear complexes with L = 2,2′-bipy (1.959 Å, 100 K), phen (1.992 Å, 130 K), btz (1.965 Å, 130 K), bt (1.951 Å, 150 K) and TAP (1.967 Å, 135 K) and is consistent with the LS state of the Fe^{II} centre. A similar conclusion can be inferred from the angular distortion values of the $[FeN_6]$ octahedron Σ and Φ (see Table 3). The major difference between these monomeric complexes and **1·(1.5MeOH)** is the 1D polymeric nature of the latter with the Fe^{II} ions linked through the rigid ligand HAT within a chain. This rigidity could be, in part, responsible for the stronger ligand field felt by the Fe^{II} centres and hence of the high average T_c value, *ca.* 300 K, observed for the SCO **1·(1.5MeOH)** compared to that of the aforementioned monomeric compounds [L = TAP (165 K), phen (174 K), bt (180 K), 2,2′-bipy (215 K), btz (227 K)]. It is particularly relevant the large difference of T_c values observed for the complexes **1·(1.5MeOH)** and $[Fe(TAP)_2(NCS)_2]\cdot CH_3CN$ (solvate

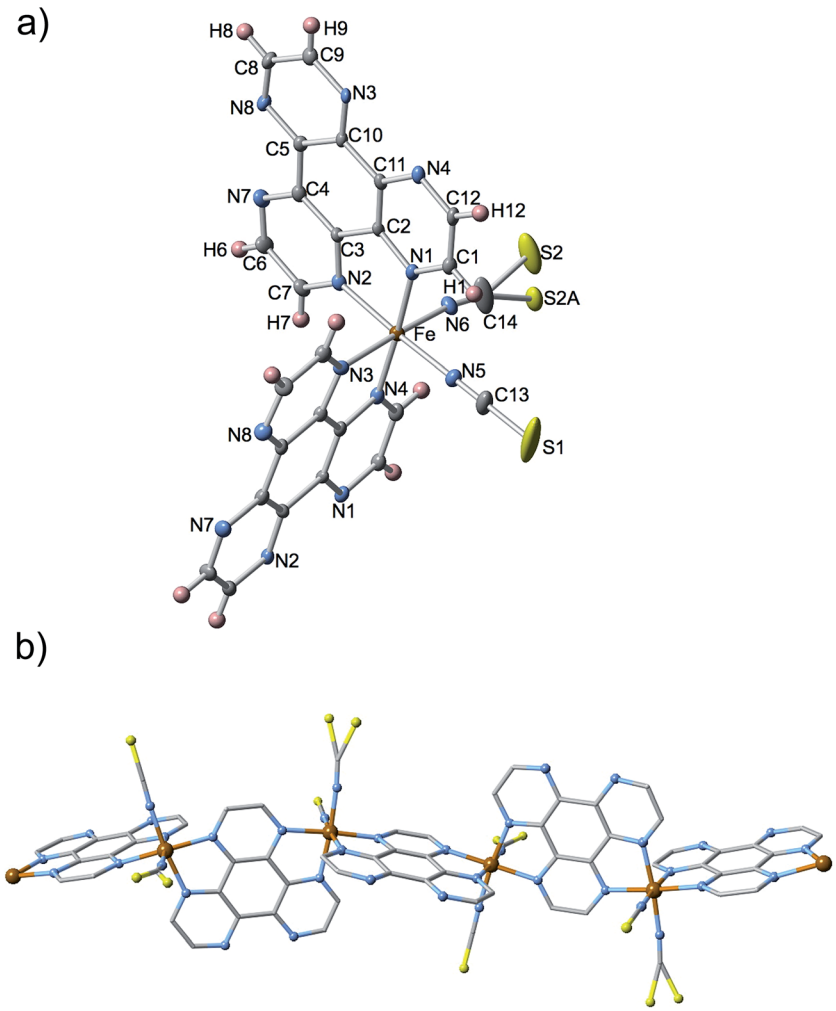

Fig. 1 ORTEP representation of the coordination site (thermal ellipsoids are represented at 30% probability) (a) and fragment of the chain (b) of **1·(1.5MeOH)**. The sulphur atom of the NCS^- anion is disordered and has been solved in two positions.

A), despite the close similarities between the HAT and TAP ligands. However, it is well known that the crystal packing also plays an important role in the modulation of the ligand field. For example, in contrast to solvate A the solvate B $[Fe(TAP)_2(NCS)_2]\cdot 1/2CH_3CN$ crystallizes in a different space group where the Fe^{II} is much more distorted ($\Sigma = 86°$ and $\Phi = 15.8°$) and consequently solvate B is HS at all temperatures. A similar example is illustrated by the two polymorphs of $[Fe(bt)_2(NCS)_2]$. Polymorph A undergoes SCO while polymorph B with a much more distorted Fe^{II} geometry ($\Sigma = 85°$ and $\Phi = 14.7°$) is HS. Note the particularly large Φ values exhibited by the HS species in the last two cases (see Table 3).

Attempts to obtain single crystal data of **1·(1.5MeOH)** at 290–300 K resulted unfruitful due to deterioration of the crystals most likely due to the loss of the MeOH molecules. Indeed, above *ca.* 310 K, **1·(1.5MeOH)** irreversibly loses the solvent molecules suffering drastic structural changes, which presumably involve a closer packing of the chains. This transformation deteriorates the quality of the crystals of the unsolvate compound **1** preventing any single crystal analysis. The partial loss of crystallinity of the resulting microcrystalline power of **1** makes very difficult indexation of the powder X-ray diffraction (PXRD) data (see Fig. S3 in ESI†). However, based on the obtained values of ΔH_i and T_{ci}, the two-step SCO behaviour clearly suggests the presence of two crystallographically different Fe^{II} sites, which feel notably different ligand field strengths. Consistently, the IR spectrum of **1** at 300 K where the HS–LS population is *ca.* 56–44% (upper limit of the plateau) shows the presence of the characteristic CN stretching modes of the SCN^- group in the LS state [$\nu(CN)^{LS} = 2122$ and 2112 cm^{-1}] and the HS state [$\nu(CN)^{HS} = 2080$ and 2046 cm^{-1}] (see Fig. S4 in ESI†).[19]

Despite two-step SCO in Fe^{II} and Fe^{III} complexes is still considered a rare event, nowadays there is at least *ca.* 46 systems crystallographically characterised ranging from discrete mononuclear,[20] dinuclear,[21] and tetranuclear[22] species to one-,[23] two-[18,24] and three-dimensional[25] coordination polymers. In general the singular step is constituted of an ordered LS–HS state for symmetrical transitions but have also been described some unsymmetrical transitions with ordered LS–LS–HS[20e] or HS–HS–LS[24e] states. For a relatively small fraction of these examples (8 of 46) the spin state of the step could not be directly substantiated from direct crystallographic analysis but the

Table 3 Sum of the deviation from 90° of the 12 N–Fe–N angles (Σ°) and average trigonal distortion angle (Φ°) for related compounds (see text)

	Φ		Σ	
Compound	LS	HS	LS	HS
$Fe(phen)_2(NCS)_2$ (ref. 16a)	4.7	8.5	35	64
$Fe(btz)_2(NCS)_2$ (ref. 16b)	4.9	7.4	49	83
$Fe(TAP)_2(NCS)_2\cdot CH_3CN$[16c]	2.8	5.9	37	80
$Fe(2,2'\text{-bpy})_2(NCS)_2$ (ref. 16d)	4.8	8.7	46	65
[a]$Fe(bt)_2(NCS)_2$ (ref. 16e)	5.5	9.6	79	53
$Fe(PM\text{-}PeA)_2(NCS)_2$ (ref. 16f)	4.2	8.2	56	85
$Fe(HAT)_2(NCS)_2\cdot 1.5CH_3OH$	3.5		33	

[a] Polymorph A.

presence of the LS–HS state could be confirmed from a combination of Mössbauer spectroscopy in presence of strong magnetic field, Raman spectroscopy, single crystal X-ray diffraction and LIESST effect in one case[21a–e] or simply zero-field Mössbauer spectroscopy in another example.[21j] No observation in these cases of an intermediate ordered state may be related to the occurrence of positional disorder, thermal motion in the crystal or other causes. It is pertinent to mention here the two-step spin crossover behaviour observed in {Fe(pmd)$[Ag(CN)_2][Ag_2(CN)_3]$} (pmd = pyrimidine) because it illustrates an uncommon example where both ordered and disordered events are observed in the same crystal. This compound is constituted of three crystallographically different-Fe–pmd–Fe-infinite chains interconnected through the bridges $[Ag(CN)_2]^-$ and $[Ag_2(CN)_3]^-$. The chains contain different Fe^{II} distinguishable sites Fe(A)–pmd–Fe(B), Fe(C)–pmd–Fe(D), and Fe(E)–pmd–Fe(E). The two-step transition could be monitored from the variation of the Fe–N bond lengths. In the intermediate plateau the chains Fe(A)–pmd–Fe(B) and Fe(C)–pmd–Fe(D) show perfectly ordered HS–LS–HS–LS states while the crystallographic analysis of chain Fe(E)–pmd–Fe(E) can only afford an average of HS and LS sites.[25b] Despite this, it is reasonable to infer that in the latter chain the ordered HS–LS–HS–LS state must also exist. It should be also stressed that the presence of one or several different Fe^{II} sites is not necessary condition to observe, respectively, a single or a multi-step SCO behaviour. For example, the former case is illustrated by the paradigmatic mononuclear compound $[Fe(pic)_3]Cl_2\cdot EtOH$ (pic = picolylamine) which only has one type of Fe^{II} in the HS and LS phase but appear two Fe^{II} sites in the intermediate phase.[20a] In contrast, the one-dimensional compound $\{Fe(aqin)_2[N(CN)_2]\}(ClO_4)\cdot MeOH$ (aquin = 8-aminoquinoline) characterised by the presence of two crystallographically different Fe^{II} ions essentially displays only a single step SCO behaviour.[26] Based on most of the examples described so far, it is sensible to suggest that the two-step SCO behaviour observed for compound **1** takes place through an intermediate ordered state where the HS and LS state are alternated. However, this could only be substantiated by means of an analysis of sufficiently good crystallographic data.

Concluding remarks

Here we have described the first SCO system based on the singular C_3-symmetric tris-bidentate bridging ligand HAT. This new SCO system consists of one-dimensional homochiral chains $[Fe(HAT)(NCS)_2]_\infty\cdot n$MeOH ($n$ = 0, 1.5), which undergoes a complete two-step spin crossover behaviour. Homochirality is a rare event in the field of SCO. As far as we know, only 5 examples of chiral SCO compounds have been reported until now. The first reported homochiral SCO compound was the mononuclear mixed valence complex $[Fe^{II}(H_3L)][Fe^{III}L](NO_3)_2$ (H_3L = tris{[2-{(imidazole-4-yl) methylidene}amino]ethyl}amine)). It is worth stressing that the two Fe sites (Fe^{II} and Fe^{III}) of this compound undergo SCO behaviour.[27] More recently the same research group has reported the related mononuclear homochiral SCO compounds $[Fe^{III}(H_3L)][Fe^{III}L][Cr^{III}(C_2O_4)_3]\cdot 3H_2O$[28] and fac-Λ-$[Fe^{II}(HL^R)_3](ClO_4)_2\cdot EtOH$ (HL^R = 2-methylimidazol-4-yl-methylideneamino-R-(+)-1-methylphenyl).[29] Extension of homochirality to SCO coordination polymers has afforded the compounds (+)-{$[Fe^{II}$(4-

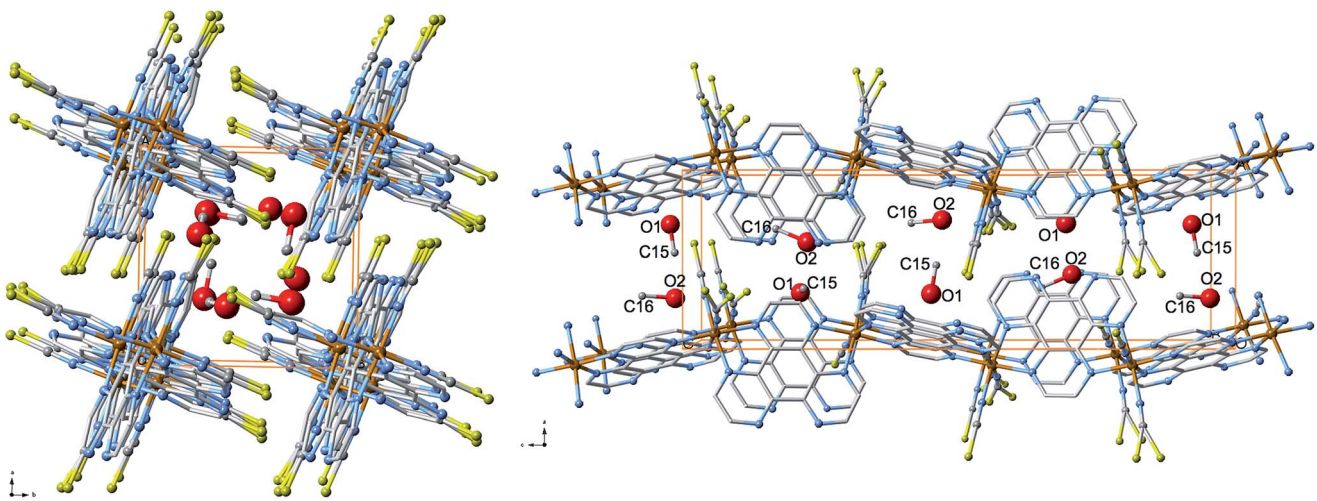

Fig. 2 Perspective views of the crystal packing of **1·(1.5MeOH)** along [001] (left) and [010] (right) directions.

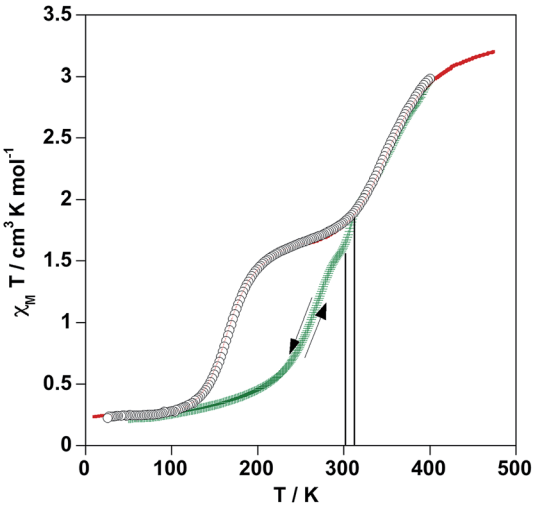

Fig. 3 Experimental $\chi_M T$ *vs.* T data for **1·(1.5MeOH)** (green crosses) and **1** (open circles), and calculated data for **1** (red line). The two vertical lines mark the temperature interval where $\chi_M T$ increases due to loss of the methanol molecules (see text). Arrows indicate a cooling–heating cycle for **1·(1.5MeOH)** without surpassing 300 K.

bromopyridine)$_4$]$_2$[Nb(CN)$_8$]}·2H$_2$O[30] and [Fe^{II}(mptpy)$_2$]·EtOH·0.2DMF (mptpy = 3-methyl-2-(5-(4-(pyridin-4-yl)phenyl)-4H-1,2,4-triazol-3-yl)-pyridine).[31] Particularly relevant is the former three-dimensional coordination polymer since it combines in a synergetic way SCO-induced second-harmonic generation (SHG), light induced magnetic ordering and photoswitching of the magnetization induced second-harmonic generation (MSHG).[30] This stimulating result is the first demonstration of interplay between chirality and SCO behaviour and represents a new paradigm in the search for new advanced materials, which justifies the synthesis and characterisation of new homochiral SCO compounds.

Experimental

Materials

Solvents and starting materials were purchased from commercial sources and used without further purification. The ligand HAT was synthesized according to the reported procedure.[32]

Synthesis of **1·(1.5MeOH)**: a solution of HAT ligand (12 mg, 0.051 mmol) in chloroform (2 mL) was poured into one side of an H-shaped diffusion tube (total volume 10 mL). A filtered solution of 1Fe^{II}: 2NCS$^-$ in methanol (2 mL), prepared in an Argon atmosphere by mixing FeSO$_4$·7H$_2$O (42.8 mg, 0.154 mmol) and KNCS (29.9 mg, 0.308 mmol) together with a few ascorbic crystals, was poured into the other side of the H-shaped tube. The tube was filled with a 1 : 1 mixture of methanol–chloroform and sealed. Needle-like single crystals of **1·(1.5MeOH)** appear after four weeks (yield: 60%). Its composition was determined by single crystal X-ray diffraction and thermal analysis.

The desolvated compound **1** was obtained by thermal treatment of **1·(1.5MeOH)** (see ESI†). Elemental analysis calcd (%) for C$_{14}$H$_6$FeN$_8$S$_2$: C, 41.39; H, 1.48; N, 27.59. Found: C, 41.63; H, 1.52; N, 27.92.

Physical measurements

Variable-temperature magnetic susceptibility data were recorded with a Quantum Design MPMS2 SQUID susceptometer equipped with a 7 T magnet, operating at 1 T and at temperatures 2–400 K. Experimental susceptibilities were corrected from diamagnetism of the constituent atoms by the use of Pascal's constants. TGA measurements were performed on a Mettler Toledo TGA/SDTA 851e, in the 290–800 K temperature range under a nitrogen atmosphere with a rate of 10 K min^{-1}. Microanalyses were performed using a LECO CHNS-932 analyser. Powder X-ray diffraction data were recorded with a Seifert XRD 3003 TT diffractometer, equipped with a Bragg–Brentano geometry, a Cu tube working at 40 kV and a Ni filter (0.3 mm primary slit, 0.3 mm secondary slit, 0.2 mm detector slit and scintillation detector). Infra-red spectra were performed using a Nicolet 5700 FT-IR spectrophotometer in the range 4000–400 cm^{-1} with the samples compressed as KBr disks.

Single-crystal X-ray data of **1·(1.5MeOH)** were collected on an Oxford Diffraction Supernova single crystal diffractometer using MoKα radiation (λ = 0.71073 Å). A data scaling and empirical or multi-scan absorption correction was performed. The structure was solved by direct methods using SHELXS-97 and refined by full-matrix least squares on F^2 using SHELXL-97.[33] Non-hydrogen atoms were refined anisotropically. Hydrogen atoms of the MeOH molecules were located by Fourier difference synthesis and remaining H atoms were geometrically placed (riding model) and assigned fixed isotropic displacement parameters. CCDC 1060123.†

Acknowledgements

The research reported here was supported by the Spanish Ministerio de Economía y Competitividad (MINECO) and FEDER funds (CTQ2013-46275-P) and Generalitat Valenciana (PROMETEO/2012/049). T.R.M. and F.J.V.M. thank the Spanish Ministerio de de Economía y Competitividad (MINECO) for a predoctoral (FPI) grant. We thank Dr José Alberto Rodriguez-Velamazán for his advice concerning the PXRD patterns.

References

1 Spin Crossover in Transition Metal Compounds I–III:*Topics in Current Chemistry*, ed. P. Gütlich and H. A. Goodwin, Springer-Verlag, Berlin, Germany, 2004, vol. 233–235.
2 *Spin-crossover materials: properties and applications*, ed. M. A. Halcrow, John Wiley & Sons, Ltd., New York, 2013.
3 C. Enachescu, M. Nishino and S. Miyashita, in *Spin-Crossover Materials: Properties and Applications*, ed. M. A. Halcrow, Wiley, 2013, pp. 455–474, references therein.
4 A. B. Gaspar, M. C. Muñoz and J. A. Real, *J. Mater. Chem.*, 2006, **16**, 2522–2533.
5 S. Ohkoshi, K. Imoto, Y. Tsunobuchi, S. Takano and H. Tokoro, *Nat. Chem.*, 2013, **3**, 564–569.
6 S. Dorbes, L. Valade, J. A. Real and C. Faulmann, *Chem. Commun.*, 2005, 69–71; C. Faulmann, K. Jacob, S. Dorbes, S. Lampert, I. Malfant, M. L. Doublet, L. Valade and

J. A. Real, *Inorg. Chem.*, 2007, **46**, 8548–8559; K. Takahashi, H. B. Cui, Y. Okano, H. Kobayashi, Y. Einaga and O. Sato, *Inorg. Chem.*, 2006, **45**, 5739–5741; K. Takahashi, H. B. Cui, Y. Okano, H. Kobayashi, H. Mori, H. Tajima, Y. Einaga and O. Sato, *J. Am. Chem. Soc.*, 2008, **130**, 6688–6689; H. Phan, S. M. Benjamin, E. Steven, J. S. Brooks and M. Shatruk, *Angew. Chem., Int. Ed.*, 2015, **54**, 823–827.

7 M. Matsuda, H. Isozaki and H. Tajima, *Thin Solid Films*, 2008, **517**, 1465–1467; L. Salmon, G. Molnár, D. Zitouni, C. Quintero, C. Bergaud, J. C. Micheau and A. Bousseksou, *J. Mater. Chem.*, 2010, **20**, 5499–5503; S. Titos-Padilla, J. M. Herrera, X. W. Chen, J. J. Delgado and E. Colacio, *Angew. Chem., Int. Ed.*, 2010, **50**, 3290–3293; Y. Garcia, F. Robert, A. D. Naik, G. Zou, B. Tinant, K. Robeyns, S. Michotte and L. Piraux, *J. Am. Chem. Soc.*, 2011, **13**, 15850–15853.

8 Selection of some relevant papers: J. A. Real, E. Andrés, M. C. Muñoz, M. Julve, T. Granier, A. Bousseksou and F. Varret, *Science*, 1995, **268**, 265–267; G. J. Halder, C. J. Kepert, B. Moubaraki, K. S. Murray and J. D. Cashion, *Science*, 2002, **298**, 1762–1765; S. M. Neville, B. Moubaraki, K. S. Murray and C. J. Kepert, *Angew. Chem., Int. Ed.*, 2007, **46**, 2059–2062; S. M. Neville, G. J. Halder, K. W. Chapman, M. B. Duriska, P. D. Southon, J. D. Cashion, J. F. Létard, B. Moubaraki, K. S. Murray and C. J. Kepert, *J. Am. Chem. Soc.*, 2008, **130**, 2869–2876; M. Ohba, K. Yoneda, G. Agustí, M. C. Muñoz, A. B. Gaspar, J. A. Real, M. Yamasaki, H. Ando, Y. Nakao, S. Sakaki and S. Kitagawa, *Angew. Chem., Int. Ed.*, 2009, **48**, 4767–4771; G. Agustí, R. Ohtani, K. Yoneda, A. B. Gaspar, M. Ohba, J. F. Sánchez-Royo, M. C. Muñoz, S. Kitagawa and J. A. Real, *Angew. Chem., Int. Ed.*, 2009, **48**, 8944–8947; P. D. Southon, L. Liu, E. A. Fellows, D. J. Price, G. J. Halder, K. W. Chapman, B. Moubaraki, K. S. Murray, J. F. Létard and C. J. Kepert, *J. Am. Chem. Soc.*, 2009, **131**, 10998–11009; Z. Arcís-Castillo, F. J. Muñoz-Lara, M. C. Muñoz, D. Aravena, A. B. Gaspar, J. F. Sánchez-Royo, E. Ruiz, M. Ohba, R. Matsuda, S. Kitagawa and J. A. Real, *Inorg. Chem.*, 2013, **52**, 12777–12783; L. Piñeiro-López, M. Seredyuk, M. C. Muñoz and J. A. Real, *Chem. Commun.*, 2014, **50**, 1833–1835.

9 S. Hayami, in *Spin-Crossover Materials: Properties and Applications*, ed. M. A. Halcrow, Wiley, 2013, pp. 376–404, references therein.

10 V. Meded, A. Bagrets, K. Fink, R. Chandrasekar, M. Ruben, F. Evers, A. Bernand-Mantel, J. S. Seldenthuis, A. Beukman and H. S. J. van der Zant, *Phys. Rev. B: Condens. Matter Mater. Phys.*, 2011, **83**, 245415; F. Prins, M. Monrabal-Capilla, E. A. Osorio, E. Coronado and H. S. J. van der Zant, *Adv. Mater.*, 2011, **23**, 1545–1549; M. Cavallini, I. Bergenti, S. Milita, J. C. Kengne, D. Gentili, G. Ruani, I. Salitros, V. Meded and M. Ruben, *Langmuir*, 2011, **27**, 4076–4081; T. Miyamachi, M. Gruber, V. Davesne, M. Bowen, S. Boukari, L. Joly, F. Scheurer, G. Rogez, T. K. Yamada, P. Ohresser, E. Beaurepaire and W. Wulfhekel, *Nat. Commun.*, 2012, **3**, 938; P. N. Martinho, C. Rajnak and M. Ruben, in *Spin-Crossover Materials: Properties and Applications*, ed. M. A. Halcrow, Wiley, 2013, pp. 376–404, references therein; H. J. Shepherd, G. Molnár, W. Nicolazzi, L. Salmon and A. Bousseksou, *Eur. J. Inorg. Chem.*, 2013, 653–661; A. Rotaru, J. Dugay, R. P. Tan, I. A. Gural'skiy, L. Salmon, P. Demont, J. Carrey, G. Molnár, M. Respaud and A. Bousseksou, *Adv. Mater.*, 2013, **25**, 1745–1749; I. A. Gural'skiy, C. M. Quintero, J. Sánchez Costa, P. Demont, G. Molnár, L. Salmon, H. J. Shepherd and A. Bousseksou, *J. Mater. Chem. C*, 2014, **2**, 2949–2955; C. Bartual Murgui, A. Akou, C. Thibault, G. Molnár, C. Vieu, L. Salmon and A. Bousseksou, *J. Mater. Chem. C*, 2015, **3**, 1277–1285.

11 S. Kitagawa and S. Masaoka, *Coord. Chem. Rev.*, 2003, **243**, 73–88.

12 M. Shatruk, A. Chouai, A. V. Prosvirin and K. R. Dunbar, *Dalton Trans.*, 2005, 1897–1902.

13 J. R. Galán-Mascarós and K. R. Dunbar, *Chem. Commun.*, 2001, 217–218; S. R. Marshall, A. L. Rheingold, L. N. Dawe, W. W. Shum, C. Kitamura and J. S. Miller, *Inorg. Chem.*, 2002, **41**, 3599–3601.

14 H. Grove, J. Sletten, M. Julve, F. Lloret, L. Lezama, J. Carranza, S. Parsons and P. Rillema, *J. Mol. Struct.*, 2002, **606**, 253; H. Grove, J. Sletten, M. Julve and F. Lloret, *J. Chem. Soc., Dalton Trans.*, 2001, 1029–1034.

15 J. A. Real, M. C. Muñoz, E. Andrés, T. Granier and B. Gallois, *Inorg. Chem.*, 1994, **33**, 3587–3594.

16 (*a*) B. Gallois, J. A. Real, C. Hauw and J. Zarembowitch, *Inorg. Chem.*, 1990, **29**, 1152–1158; (*b*) J. A. Real, B. Gallois, T. Granier, F. Suez-Panamá and J. Zarembowitch, *Inorg. Chem.*, 1992, **31**, 4972–4979; (*c*) J. A. Real, M. C. Muñoz, E. Andrés, T. Granier and B. Gallois, *Inorg. Chem.*, 1994, **33**, 3587–3594; (*d*) M. Konno and M. M. Kido, *Bull. Chem. Soc. Jpn.*, 1991, **64**, 339–345; (*e*) A. Galet, A. B. Gaspar, M. C. Muñoz, G. Levchenko and J. A. Real, *Inorg. Chem.*, 2006, **45**, 9670–9679; (*f*) J. F. Létard, P. Guionneau, E. Codjovi, O. Lavastre, G. Bravic, D. Chasseau and O. Kahn, *J. Am. Chem. Soc.*, 1997, **119**, 10861–10862.

17 C. P. Slichter and H. G. Drickamer, *J. Chem. Phys.*, 1972, **56**, 2142–2143.

18 X. Bao, P.-H. Guo, W. Liu, J. Tucek, W.-X. Zhang, J.-D. Leng, X.-M. Chen, I. Gural'skiy, L. Salmon, A. Bousseksou and M.-L. Tong, *Chem. Sci.*, 2012, **3**, 1629–1633.

19 (*a*) E. König and K. Madeja, *Spectrochim. Acta*, 1967, **23A**, 45–54; (*b*) M. Sorai and S. Seki, *J. Phys. Chem. Solids*, 1974, **33**, 555–570.

20 (*a*) D. Chernyshov, M. Hostettler, K. W. Törnroos and H. B. Bürgi, *Angew. Chem., Int. Ed.*, 2003, **42**, 3825–3830; (*b*) D. Boinnard, A. Bousseksou, A. Dworkin, J. M. Savariault, F. Varret and J. P. Tuchagues, *Inorg. Chem.*, 1994, **33**, 271; (*c*) B. A. Leita, S. M. Neville, G. J. Halder, B. Moubaraki, C. J. Kepert, J. F. Letard and K. S. Murray, *Inorg. Chem.*, 2007, **46**, 8784–8795; (*d*) M. S. Shongwe, B. A. Al-Rashdi, H. Adams, M. J. Morris, M. Mikuriya and G. R. Hearne, *Inorg. Chem.*, 2007, **46**, 9558–9568; (*e*) S. Bonnet, M. A. Siegler, J. Sanchez Costa, G. Molnár, A. Bousseksou, A. L. Spek, P. Gamez and J. Reedijk, *Chem. Commun.*, 2008, 5619–5621; (*f*) T. Sato, K. Nishi, S. Iijima, M. Kojima and N. Matsumoto, *Inorg. Chem.*, 2009, **48**, 7211–7229; (*g*)

J. Tang, J. Sánchez Costa, S. Smulders, G. Molnár, A. Bousseksou, S. J. Teat, Y. Li, G. A. van Albada, P. Gamez and J. Reedijk, *Inorg. Chem.*, 2009, **48**, 2128–2135; (*h*) N. Bréfuel, H. Watanabe, L. Toupet, J. Come, N. Matsumoto, E. Collet, K. Tanaka and J. P Tuchagues, *Angew. Chem., Int. Ed.*, 2009, **48**, 9304–9307; (*i*) J. Klingele, D. Kaase, M. H. Klingele, J. Lach and S. Demeshko, *Dalton Trans.*, 2010, **39**, 1689–1691; (*j*) M. Griffin, S. Shakespeare, H. J. Shepherd, C. J. Harding, J. F. Létard, C. Desplanches, A. E. Goeta, J. A. K. Howard, A. K. Powell, V. Mereacre, Y. Garcia, A. D. Naik, H. Müller-Bunz and G. G. Morgan, *Angew. Chem., Int. Ed.*, 2011, **50**, 896–900; (*k*) Z.-Y. Li, J.-W. Dai, Y. Shiota, K. Yoshizawa, S. Kanegawa and O. Sato, *Chem.–Eur. J.*, 2013, **19**, 12948–12952; (*l*) Z.-Y. Li, J.-W. Dai, K. J. Gagnon, H.-L. Cai, T. Yamamoto, Y. Einaga, H.-H. Zhao, S. Kanegawa, O. Sato, K. R. Dunbar and R.-G. Xiong, *Dalton Trans.*, 2013, **42**, 14685–14688; (*m*) B. J. C. Vieira, J. T. Coutinho, I. C. Santos, L. C. J. Pereira, J. C. Waerenborgh and V. da Gama, *Inorg. Chem.*, 2013, **52**, 3845–3850; (*n*) J. Luan, J. Zhou, Z. Liu, B. Zhu, H. Wang, X. Bao, W. Liu, M.-L. Tong, G. Peng, H. Peng, L. Salmon and A. Bousseksou, *Inorg. Chem.*, 2015, **54**, 5145–5147; (*o*) D. J. Harding, W. Phonsri, P. Harding, K. S. Murray, B. Moubaraki and G. N. L. Jameson, *Dalton Trans.*, 2015, DOI: 10.1039/c4dt03184a.

21 (*a*) J. A. Real, H. Bolvin, A. Bousseksou, A. Dworkin, O. Kahn, F. Varret and J. Zarembowitch, *J. Am. Chem. Soc.*, 1992, **114**, 4650–4658; (*b*) V. Ksenofontov, H. Spiering, S. Reiman, Y. Garcia, A. B. Gaspar, N. Moliner, J. A. Real and P. Gütlich, *Chem. Phys. Lett.*, 2001, **348**, 381–386; (*c*) A. B. Gaspar, V. Ksenofontov, S. Reiman, P. Gütlich, A. L. Thompson, A. E. Goeta, M. C. Muñoz and J. A. Real, *Chem.–Eur. J.*, 2006, **12**, 9289–9298; (*d*) N. Ould Moussa, G. Molnár, S. Bonhommeau, A. Zwick, S. Mouri, K. Tanaka, J. A. Real and A. Bousseksou, *Phys. Rev. Lett.*, 2005, **94**, 107205; (*e*) E. Trzop, M. Buron-Le Cointe, H. Cailleau, L. Toupet, G. Molnár, A. Bousseksou, A. B. Gaspar, J. A. Real and E. Collet, *J. Appl. Crystallogr.*, 2007, **40**, 158–164; (*f*) M. H. Klingele, B. Moubaraki, J. D. Cashion, K. S. Murray and S. Brooker, *Chem. Commun.*, 2005, 987–989; (*g*) K. Nakano, S. Kawata, K. Yoneda, A. Fuyuhiro, T. Yagi, S. Nasu, S. Morimoto and S. Kaizaki, *Chem. Commun.*, 2004, 2892–2893; (*h*) N. Ortega-Villar, A. L. Thompson, M. C. Muñoz, V. M. Ugalde-Saldívar, A. E. Goeta, R. Moreno-Esparza and J. A. Real, *Chem.–Eur. J.*, 2005, **11**, 5721–5734; (*i*) J. J. M. Amoore, C. J. Kepert, J. D. Cashion, B. Moubaraki, S. M. Neville and K. S. Murray, *Chem.–Eur. J.*, 2006, **12**, 8220–8227; (*j*) A. Y. Verat, N. Ould-Moussa, E. Jeanneau, B. Le Guennic, A. Bousseksou, S. A. Borshch and G. S. Matouzenko, *Chem.–Eur. J.*, 2009, **15**, 10070–10082; (*k*) T. Sato, K. Nishi, S. Iijima, M. Kojima and N. Matsumoto, *Inorg. Chem.*, 2009, **48**, 7211–7229; (*l*) G. S. Matouzenko, E. Jeanneau, A. Y. Verat and A. Bousseksou, *Dalton Trans.*, 2011, 9608–9618.

22 (*a*) M. Nihei, M. Ui, M. Yokota, L. Han, A. Maeda, H. Kishida, H. Okamoto and H. Oshio, *Angew. Chem., Int. Ed.*, 2005, **44**, 6484–6487; (*b*) R.-J. Wei, Q. Huo, J. Tao, R.-B. Huang and L.-S. Zheng, *Angew. Chem., Int. Ed.*, 2011, **50**, 8940–8943.

23 (*a*) W. Bauer, T. Pfaffeneder, K. Achterhold and B. Weber, *Eur. J. Inorg. Chem.*, 2011, 3183–3192; (*b*) G. S. Matouzenko, D. Luneau, G. Molnár, N. Ould-Moussa, S. Zein, S. A. Borshch, A. Bousseksou and F. Averseng, *Eur. J. Inorg. Chem.*, 2006, 2671–2682.

24 (*a*) M. C. Muñoz, A. B. Gaspar, A. Galet and J. A. Real, *Inorg. Chem.*, 2007, **46**, 8182–8192; (*b*) G. J. Halder, K. W. Chapman, S. M. Neville, B. Moubaraki, K. S. Murray, J. F. Létard and C. J. Kepert, *J. Am. Chem. Soc.*, 2008, **130**, 17552–17562; (*c*) G. Agustí, M. C. Muñoz, A. B. Gaspar and J. A. Real, *Inorg. Chem.*, 2008, **47**, 2552–2561; (*d*) V. Martínez, A. B. Gaspar, M. C. Muñoz, G. V. Bukin, G. Levchenko and J. A. Real, *Chem.–Eur. J.*, 2009, **15**, 10960–10971; (*e*) G. Agustí, A. B. Gaspar, M. C. Muñoz, P. G. Lacroix and J. A. Real, *Aust. J. Chem.*, 2009, **62**, 1155–1165; (*f*) C. J. Adams, M. C. Muñoz, R. E. Waddington and J. A. Real, *Inorg. Chem.*, 2011, **50**, 10633–10642; (*g*) J.-B. Lin, W. Xue, B.-Y. Wang, J. Tao, W.-X. Zhang, J.-P. Zhang and X.-M. Chen, *Inorg. Chem.*, 2012, **51**, 9423–9430.

25 (*a*) Y. Garcia, O. Kahn, L. Rabardel, B. Chansou, L. Salmon and J. P. Tuchagues, *Inorg. Chem.*, 1999, **38**, 4663–4670; (*b*) V. Niel, A. L. Thompson, A. E. Goeta, C. Enachescu, A. Hauser, A. Galet, M. C. Muñoz and J. A. Real, *Chem.–Eur. J.*, 2005, **11**, 2047–2060; (*c*) G. Agustí, A. B. Gaspar, M. C. Muñoz and J. A. Real, *Inorg. Chem.*, 2007, **46**, 9646–9654; (*d*) J. A. Rodríguez-Velamazán, C. Carbonera, M. Castro, E. Palacios, T. Kitazawa, J. F. Létard and R. Burriel, *Chem. Eur. J.*, 2010, **16**, 8785–8796; (*e*) N. F. Sciortino, K. R. Scherl-Gruenwald, G. Chastanet, G. J. Halder, K. W. Chapman, J. F. Létard and C. J. Kepert, *Angew. Chem., Int. Ed.*, 2012, **51**, 10154–10158; (*f*) Y. M. Klein, N. F. Sciortino, F. Ragon, C. E. Housecroft, C. J. Kepert and S. M. Neville, *Chem. Commun.*, 2014, **50**, 3838–3840; (*g*) L. Piñeiro-López, M. Seredyuk, M. C. Muñoz and J. A. Real, *Chem. Commun.*, 2014, **50**, 1833–1835.

26 C. Genre, E. Jeanneau, A. Bousseksou, D. Luneau, S. A. Borshch and G. S. Matouzenko, *Chem.–Eur. J.*, 2008, **14**, 697–705.

27 Y. Sunatsuki, Y. Ikuta, N. Matsumoto, H. Ohta, M. Kojima, S. Iijima, S. Hayami, Y. Maeda, S. Kaizaki, F. Dahan and J. P. Tuchagues, *Angew. Chem., Int. Ed.*, 2003, **42**, 1614–1618.

28 T. Hashibe, T. Fujinami, D. Furusho, N. Matsumoto and Y. Sunatsuki, *Inorg. Chim. Acta*, 2011, **375**, 338–342.

29 Y. Sunatsuki, S. Miyahara, Y. Sasaki, T. Suzuki, M. Kojimaa and N. Matsumoto, *CrystEngComm*, 2012, **14**, 6377–6380.

30 S. Ohkoshi, S. Takano, K. Imoto, M. Yoshikiyo, A. Namai and H. Tokoro, *Nat. Photonics*, 2014, **8**, 65–71.

31 W. Liu, X. Bao, L. L. Mao, J. Tucek, R. Zboril, J. L. Liu, F. S. Guo, Z. P. Nia and M. L. Tong, *Chem. Commun.*, 2014, **50**, 4059–4061.

32 (*a*) J. T. Rademacher, K. Kanakarajan and A. W. Czarnik, *Synthesis*, 1994, 378–380; (*b*) M. S. P. Sarma and A. W. Czarnik, *Synthesis*, 1988, 72–73.

33 G. M. Sheldrick, *Acta Crystallogr., Sect. A: Found. Crystallogr.*, 2008, **64**, 112–122.